AD NUMBER

AD350190

CLASSIFICATION CHANGES

TO: unclassified

FROM: confidential

LIMITATION CHANGES

TO:

Approved for public release, distribution unlimited

FROM:

DoD Controlling Organization...U.S. Naval Research Laboratory, Washington, DC. 20375-5320.

AUTHORITY

NRL ltr, 1 Jan 2001.; Same.

AD- 350190

SECURITY REMARKING REQUIREMENTS

DOD 5200.1-R, DEC 78

REVIEW ON 04 MAY 84

NRL Report 6046

Studies of the Ocean's Surface

Part 3 – The Detection of Surface Films and Hydrodynamic Smoothing by Sun-Glitter Photography

[UNCLASSIFIED TITLE]

K. G. WILLIAMS

Fuels Branch
Chemistry Division

May 4, 1964

U.S. NAVAL RESEARCH LABORATORY
Washington, D.C.

DDC AVAILABILITY NOTICE

Qualified requesters may obtain copies of this report from DDC.

PREVIOUS REPORTS IN THIS SERIES

"Part 1 – Laboratory Studies of Upwellings and Surface Motion," K. G. Williams, NRL Report 5757, March 1962 (Confidential Report)

"Part 2 – On the Nature of Turbulent Wakes of Ships and Submarines and Their Effects on the Surface of the Sea," K. G. Williams, NRL Report 5854, December 1962 (Confidential Report)

SECURITY

This document contains information affecting the national defense of the United States within the meaning of the Espionage Laws, Title 18, U.S.C., Sections 793 and 794. The transmission or the revelation of its contents in any manner to an unauthorized person is prohibited by law.

CONTENTS

CONTENTS

ABSTRACT
[Unclassified]

The use of sun-glitter photography to detect monomolecular layers of organic material on water surfaces through their damping effect on short water waves is discussed. Since the method is nondiscriminating, damping caused by either aerodynamic or hydrodynamic effects is also detected. Two photographically relevant parameters are the slope and the radius of curvature of the water surface. Where the predominant slope components are associated with wavelengths short enough to be effectively damped, areas of compacted surface films can be detected with a nearly infinite signal-to-noise ratio. Where major slope components are associated with longer waves not susceptible to damping, the signal-to-noise ratio deteriorates. Under adverse ocean conditions, changes of the average radius of curvature can sometimes be used to indicate areas of damping which are otherwise not readily detected.

PROBLEM STATUS

This is an interim report; work on this problem is continuing.

AUTHORIZATION

NRL Problem C02-18C
Project RUDC 4B-001/65N/SO31-01-00-231-3

Manuscript submitted November 18, 1963.

STUDIES OF THE OCEAN'S SURFACE

PART 3 - THE DETECTION OF SURFACE FILMS AND HYDRODYNAMIC SMOOTHING BY SUN-GLITTER PHOTOGRAPHY

[Unclassified Title]

INTRODUCTION

In various oceanographic problems, a knowledge of the distribution and physical characteristics of surface slicks caused by monomolecular (or thicker) films of organic material floating on the sea surface is of interest. While such films can be detected by measuring (a) the surface tension of the water, (b) the electrode potential of the surface, or (c) by chemical assay, such measurements are difficult to conduct in the field and must be made on a point-to-point basis. The slowness of this type of sampling precludes rapid time-sequential mapping of changes in the size and distribution of slicks, and it has been necessary to develop a more rapid survey technique for use in connection with studies related to detection of surface effects caused by submerged submarines.

To obtain a rapid survey technique, advantage has been taken of the well-known propensity of compacted monolayers to preferentially damp the smaller, steeper components of the wave structure of the sea. The optical effects of such damping are evident to even the most casual observer of the sea surface, even though the film which causes the damping may be confined to a surface layer less than 1/100th of the wavelength of visible light and thus be completely invisible in itself. These optical effects are recorded by photographing the glitter pattern resulting from reflections of the sun by the ocean waves.

In order to eliminate the variables of casual observation and to emphasize the differences between slick and clean areas, it has been necessary to examine the nature of the changes caused by slicks and their relation to the photographic process. This report points out some of the elementary optical considerations involved, relates the photographic image to the structure of the sea, and illustrates some results. The discussion is centered on the relatively simple case of light from a discrete source–the sun–even though slicks sometimes show up more clearly in photographs taken with extended but variegated light sources such as a cloudy sky (Fig. 1).

While the ideas contained in this report are derived from the work of many authors, specific contributions are not generally noted. A bibliography is appended which recognizes the author's source material and to which the reader is referred for more detailed treatment.

OPTICAL PRINCIPLES–WAVE SLOPE EFFECTS

When parallel beams of light from an infinitely distant point light source are reflected from a plane surface, the angles of incidence i_θ and reflection r_θ of each beam are equal. Thus, in the situation sketched in Fig. 2 (a), only one of the indicated beams will pass through the camera lens, and a single image results. The line normal to the reflecting surface at the point of reflection is the bisector of angle SRC. Where this bisector is vertical, the angle of tilt τ of the reflecting surface is defined as zero. If the plane of Fig. 2 (a) is replaced with an undulating surface which remains normal to the plane of

Fig. 1 – Wind-ruffled water surface in abandoned quarry at Halitown, W. Va., showing the normal visual contrast between film-covered and clean areas

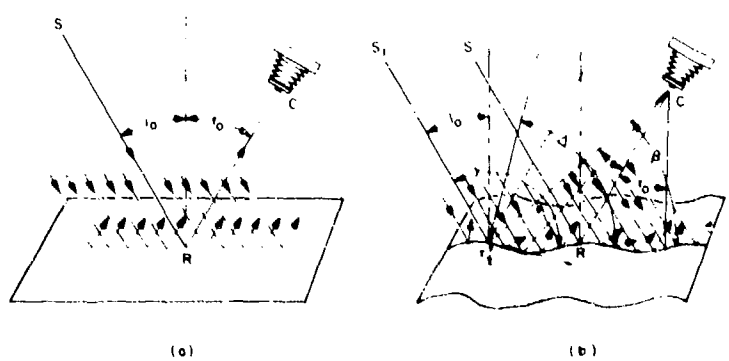

Fig. 2 – Path of light rays from infinitely distant point source reflected from (a) plane surface and (b) undulating surface normal to plane SRC

SRC, several reflected beams can pass through the lens. These will fall on the line defined by the intersection of the plane SRC and the focal plane of the camera (Fig. 2 (b)). The direction of the ray which forms any image with respect to the direction of the ray from a reflecting surface of zero tilt defines the angle α, and the tilt of the reflecting facet from which any image occurred is $\tau = \alpha/2$.

If the undulating surface is not always normal to the plane SRC, reflections can enter the lens along a path such as S'R'C (Fig. 3). In this case, the tilt τ of the facet from which the reflection occurred is the vector sum of the two angles τ_x and τ_y, which are scalarly related as follows:

$$\cos \tau = \cos \tau_x \cos \tau_y$$

where $\tau_x = \alpha_x/2$ and $\tau_y = \alpha_y/2$. As a consequence of this relationship, the locus of the instantaneous position of all possible reflecting facets for which τ is single valued forms a closed figure. In the simple case where the camera and light source lie on a common axis perpendicular to the median plane of the surface, the loci for various values of τ are circles concentric with the optical axis (Fig. 4 (a)). The path of all beams reflected from facets with the same value of τ therefore lie on the surface of a cone with its apex at the lens. At the surface, the radius r of the locus for a tilt value τ is given by $r = h \tan 2\tau$, where h is the camera elevation.

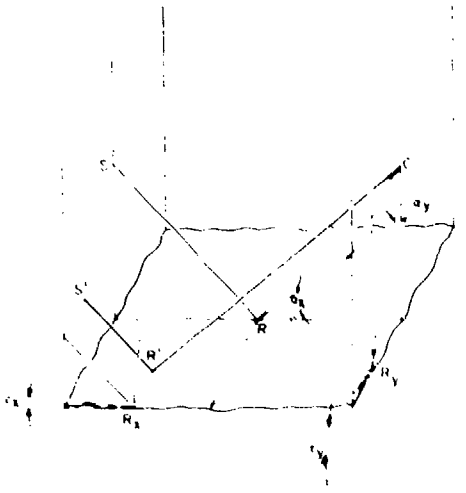

Fig. 3 – Path of light rays reflected from undulating surface not everywhere normal to plane SRC

The effect of separating the lens and light source from a common axis can be visualized as a rotation of the apex of the reflected cone of beams about an axis in the median plane of the surface and normal to the plane S_1RC_1 (Fig. 4 (b)). At the reflecting surface, the locus of facets of single-valued tilt τ becomes elliptical. By making the angle of the optical axis of the camera the same as the angle of the ray reflected from the median plane of zero tilt, reflections from facets of a single value of τ continue to fall in circles on the

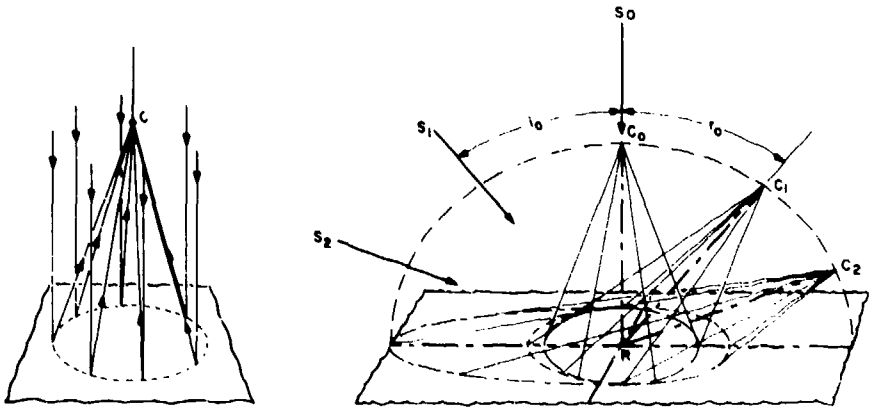

Fig. 4 – Locus of paths of light rays reflected from facets having the same tilt angle τ for (a) camera axis and infinitely distant point light source both on line normal to median plane of surface, and (b) camera axis and light source at various positions not on the normal line (vertical)

film plane, though the projection of the surface on the film plane is foreshortened. If the camera angle is not held at this angle, the film-plane locus also becomes distorted into an ellipse. If the curvature of the earth's surface is taken into consideration, computation of the film-plane loci for various tilt angles becomes even more tedious.

As a practical matter, the result of this elliptical symmetry is that sun-glitter photographs taken with a framing camera contain reflections from facets of many varying angles. Since the distribution of facets and, to some extent, the radius of curvature vary with respect to facet angle, the resulting pictures may show density anomalies which make interpretation difficult. For example, a long narrow slick running across the center of a reflection ellipse will usually show up as darker than the background at the edges, lighter than the background in the center, and of the same average density in an intermediate transition region. The reasons for this will be discussed later.

To eliminate such density anomalies, it is desirable to make the photographic presentation homogeneous in terms of facet angle. One method of approaching this goal is to limit the field of view of the camera so only a narrow range of facet angles can reflect light to the film. While this results in a loss of area coverage, this can be compensated by taking the pictures from a higher altitude. A second method, which also eliminates the foreshortening associated with nonvertical framing cameras, is to use a conventional aerial moving-film strip camera (Fig. 5). Such cameras are flown over the target area on a straight line at constant elevation from the median plane. The viewing angle is fixed with respect to the vertical. The images of individual points on the target move past a constantly open slit, behind which the film travels at a rate matched to the rate of image movement. Since the viewing angle remains constant, all reflections recorded along any line parallel to the line of flight come from facets having a single-valued tilt. However, this is not the case along the film coordinate normal to the line of flight, where the same considerations noted earlier for the framing camera apply.

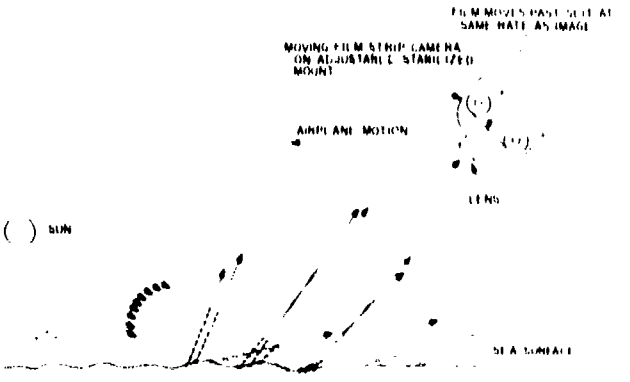

Fig. 5 – Schematic representation of aerial moving-film strip camera. As camera is flown toward the sun, only reflections from wave facets of a specific angle pass through the camera slit. Thus by tilting the camera as the sun moves, the facet angle may be held constant at any desired value.

As an aid in visualizing the distribution of facet reflection angles across the width of the film, the constructions shown in Fig. 6 are useful. In Fig. 6 (a) each of the concentric circles represents the locus of the position of facets of single-valued tilt for the case where the camera axis and an infinitely distant light source both lie on a common normal to the median plane of the surface. The radius of each circle on the figure is proportional to the tangent of twice the facet tilt angle. With the optical axis of the camera normal to the median sea surface, the field of view of the slit is represented by line AA'; and the distribution of facet tilt angles across the film is represented by the intersection of the circles designated "facet tilt" with AA'.

If the camera axis is tilted from the normal, the geographic limits of the field of view at the surface expand and the limiting facet tilt must be computed from the cosine law $\cos\gamma = (\cos\gamma_s 2)(\cos\gamma_v 2)$. When these computed values of the limiting facet tilts (in degrees) are plotted as a function of the camera tilt angle, they yield the two curves shown in Fig. 6 (b) as the heavy lines BB and B'B'.

The space between these limiting facet angle boundaries has been divided into ten equal parts, which represent equal increments across the slit. By superimposing the limiting facet angle boundary curves on the tangent circles (Fig. 6 (c)), the distribution of facet angles across the field of view can be estimated. The placement in Fig. 6 (c) corresponds to a solar elevation of 60 degrees (sun directly overhead). The distribution of facet angles is indicated by the intersections of the circles with any line parallel to AA' drawn between BB and B'B' at the appropriate camera tilt angle.

For other sun elevation angles γ_s, the line AA' must be shifted horizontally so that it is tangent to the circle corresponding to the appropriate solar elevation. This manipulation

*In Fig. 6, AA' is drawn for a camera having a field of view of 5°.

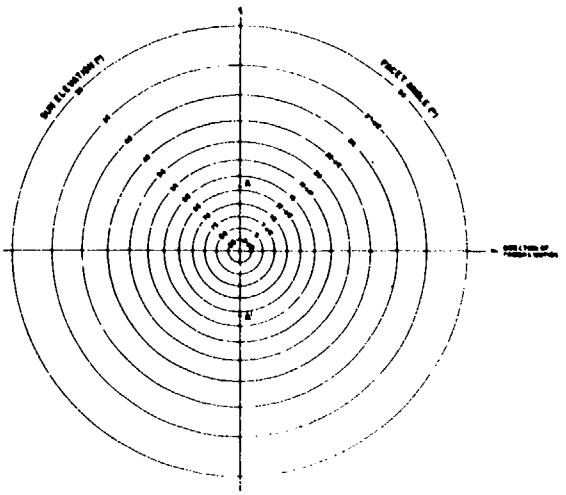

(a)

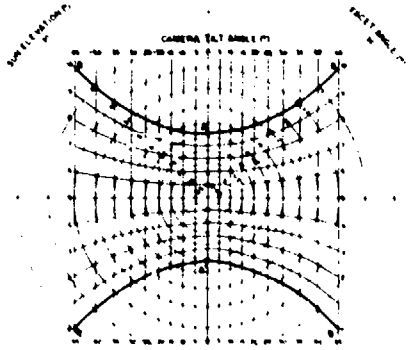

(c)

Fig. 6 – Aids for estimating the facet angle from which images were recorded across the width of film in strip camera: (a) for viewing angle and solar elevation angle both 90°, slit field of view is line AA'; (b) variations of geographic limits of field of view as a function of camera tilt angle (the maximum geographic limits for the camera used are the lines BB and B'B'); (c) superposition of (a) and (b) so that facet angles across field of view can be estimated for solar elevation of 90° and various camera tilt angles (for example, at a camera tilt angle of 40°, facet angles across the width of film range from 20° to 25°); and (d) position of grids (a) and (b) for solar elevation of 60°

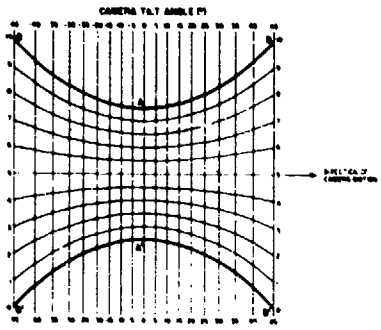

(b)

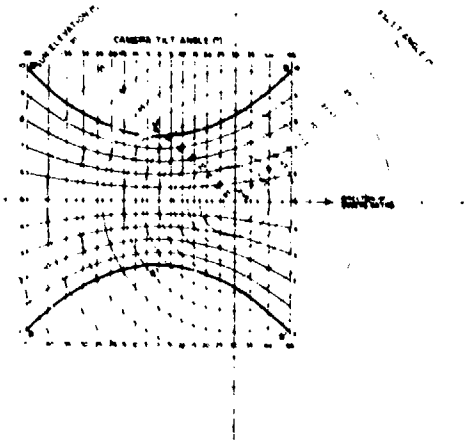

(d)

Fig. 6 (Cont'd) – Aids for estimating the facet angle from which images were recorded across the width of film in strip camera: (a) for viewing angle and solar elevation angle both 90°, slit field of view is line AA'; (b) variations of geographic limits of field of view as a function of camera tilt angle (the maximum geographic limits for the camera used are the lines BB and B'B'); (c) superposition of (a) and (b) so that facet angles across field of view can be estimated for solar elevation of 90° and various camera tilt angles (for example, at a camera tilt angle of 40°, facet angles across the width of film range from 20° to 25°); and (d) position of grids (a) and (b) for solar elevation of 60°

is shown in Fig. 6 (d) for a solar elevation of 60 degrees. The facet distribution is then found on the line parallel to AA' (drawn from BB to B'B') corresponding to the appropriate camera tilt angle. Corrections for deviations between the line of flight and the azimuth angle of the sun can also be made by rotating the overlay about the midpoint of AA' to correspond to the angular deviation.

From these constructions, it is apparent that the range of facet angles across the width of the film can be minimized by working at facet angles as far removed from zero as the sea conditions permit, and by using narrow viewing angles. In principle, the presentation could be made completely uniform through the use of slits curved to match the film plane locus of reflections from facets of single valued tilt.

IMAGE FORMATION

Framing Camera

Thus far the discussion has assumed a point source of light and, therefore, point images on the film. In sun-glitter photography, each image recorded on the film is a reflected image of a distant, extended light source, and so is of finite size. The size of such images, reflected from a plane surface, is determined by the angular aspect of the source and the focal length of the lens (Fig. 7 (a)). Since realizable changes in camera elevation are small compared with the distance to the sun, image size is independent of the camera altitude.

When the reflection occurs from a surface with spherical curvature, the area from which reflections can reach the lens is limited to a segment of the sphere, the dimensions of which depend on the radius of curvature of the reflecting surface (Fig. 7 (b)). At the film plane this area is further reduced by the photographic scale. Because the aspect angle α_s of the sun is only 32 minutes, a facet with a radius of curvature of one inch reflects from an area about 0.002 inch in radius. At photographic scales of feasible values for survey purposes, such images will be less than the grain size of the emulsion. Some photographic factors, such as lens aberrations, clumping of grains in the emulsion, and movement of either camera or reflecting surface, contribute to the detectability of small reflections. But purely on a basis of image size, it can be expected that many reflections will be submerged in the grain structure.

An even more relevant consideration is the intensity of the reflected light. The intensity falls off rapidly as the radius of curvature of the reflecting facets decreases. Thus reflections from the smallest facets tend to be lost first on an intensity basis. This situation is further aggravated by the flat foot of the exposure-density curves for typical emulsion materials.

Movement of the reflecting facet during the period of exposure also may adversely affect the recording of reflections from facets with short radius of curvature since the effective exposure is reduced by a factor which depends on the ratio of image length to its velocity. In the framing camera, the image velocity across the film is roughly the rate of movement of the reflecting facet at the water surface divided by the photographic scale. The rate of movement of the facet is approximately, though not exactly, equal to the rate of movement of the wave itself. Since the propagation velocity of water waves increases for wavelengths both larger and smaller than a certain minimum, the smallest facets will be associated with the most unfavorable length/velocity ratios.

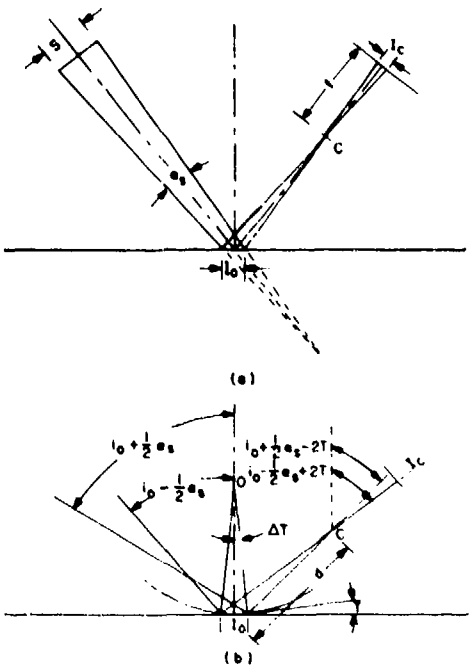

Fig. 7 – Image of finite source reflected from (a) plane surface and (b) cylindrical or spherical surface. The angular aspect of the source, α_s, l_o is size of image at surface, and l_c is recorded image size, which is equal to l_o multiplied by the photographic scale.

Strip Camera

As a consequence of both the changing viewpoint of the strip camera with time and the finite width of the slit at the focal plane, reflected images of distant sources are lines rather than points. From a plane surface of zero tilt, the image is an indefinitely long line. From undulating surfaces, images are formed by reflections from all points where the tilt τ lies within the limits $\tau_0 \pm (\alpha_a/4)$. τ_0 is the slope at which the camera is aimed, and α_a is the overall acceptance angle, which is the sum of the angular aspect of the source α_s and the acceptance angle of the camera α_c. The angle α_c is $\cot^{-1}(s/f)$, where s is the slit width measured in the direction of camera motion and f is the focal length of the lens. This can also be computed directly from the relation

$$\alpha_c = \tan^{-1}(tkv/h)\sin d,$$

where t is the exposure time in seconds, v is the camera velocity in knots, h is the altitude in feet, d is the depression angle, and k is 1.6889.

The acceptance angle concept is useful in visualizing the nature of the glitter image from a water surface. Figure 8 (a) represents the linear elevation profile of a water wave. The slope of this wave is represented by its first derivative, as shown in Fig. 8 (b). The location of reflected images on the elevation profile can therefore be determined by the intersections of the slope curve with the band $\tau_0 \pm (\alpha_a/4)$ representing the range of tilt angles which can reflect the source to the camera. Where the derivative curve crosses

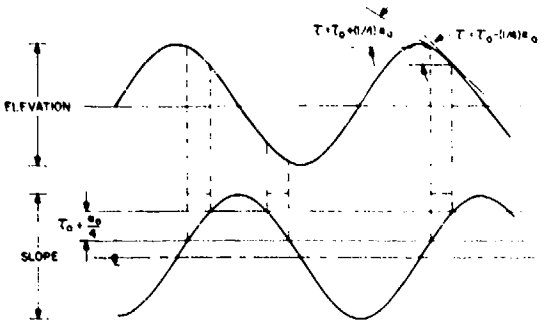

Fig. 8 – Elevation profile and slope profile of sinusoidal water wave. The viewing angle of camera, plus and minus one-quarter the overall acceptance angle α_a, is shown. Reflections are recorded on strip camera from all points on the slope curve which fall within the acceptance angle band. The vertical projections to the elevation profile indicate the areas from which reflections are recorded from the actual wave.

both limits of this band, two reflections per wave will result; where it crosses only once, only one reflection per wave is recorded. The displacement of the acceptance band from the centerline is equivalent to departure of the camera viewing angle from the elevation angle of the source.

Since the camera is moving, the effects of facet movement on the length of the recorded image are dependent on the direction of facet motion relative to the camera motion. Waves moving with the camera cause elongation of the images, while waves moving against the camera cause compression of the images. The resulting image size I can be estimated from

$$I = I_o[V_c \ (V_c + V_t)],$$

where I_o would be the image size in the absence of motion, V_c is the camera velocity, and V_t is the wave velocity. This relationship holds only for velocity components in the direction of flight and also ignores image movement resulting from change in wave shape with movement.

RELEVANT FEATURES OF THE SEA SURFACE

In the fully developed sea, the distribution of wave energy as a function of wavelength, integrated over a sufficiently long period of time to ensure statistical validity, represents a continuum which can be uniquely described as a spectral distribution. Such curves are subject to wide variations, particularly where the seas are not fully developed or are decaying, but the concept has the philosophical advantage of permitting the elevation profile of the sea to be considered as a Fourier summation which can be resolved into its various sinusoidal components. This concept is a gross oversimplification in the case of short-exposure-time

photographs where the sampled information does not represent a significant sample, but it does provide a starting point for discussion.

A typical energy spectrum is shown in Fig. 9 (a). The energy peak lies at a wavelength on the order of tens of feet. As drawn, the energy contribution of wavelengths on the order of a few inches approaches zero, but since the photographic process is sensitive only to instantaneous slope, the distribution of reflecting facets is different from the energy spectrum. If it is considered, for example, that all wavelengths of values less than n are contained in a square with an area of n^2 in phases normal to the x and y coordinates and that one reflection is associated with each wave cycle, the number of reflections for any wavelength λ would be $(n/\lambda)^2$. The distribution shown in Fig. 9 (b) would result. This distribution is not valid at any given moment of time over a finite space because of the random distribution of waveforms and because of physical limitations which make certain combinations mutually exclusive. Nevertheless, the general form of this distribution curve is qualitatively consistent with the results of direct observation, except for a falling off in the number of reflections at short wavelengths, as indicated by the dashed line. This falloff is partly due to the distribution characteristics of very small "dimples" in relation to the larger waves, but an even more significant factor is the short radius of curvature associated with the smallest waves.

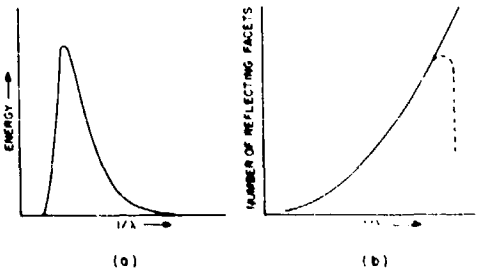

Fig. 9 — (a) Spectral distribution of energy in fully developed sea (after Pierson, see Bibliography). (b) Spectral distribution of reflecting facets for hypothetical case of long-crested waves in two phases at right angles to each other. Dotted line suggests drop observed experimentally because of discrimination against smallest facets.

As mentioned earlier, a number of photographic and physical factors combine to discriminate against the recording of reflections from very small waves, and photographs have been obtained which suggest that the smallest facets may be lost even at photographic scales of 5 to 1. As the photographic scale increases, the resolution and sensitivity both decline, and the peak in the recorded distribution curve moves to progressively longer wavelengths.

The damping effect of surface films is associated primarily with the smaller waves and results in two principal optical effects: (a) the components of the average, maximum, wave

facet tilt associated with the smaller waves are reduced, and (b) the average radius of curvature is increased. The photographic detection of slicks, therefore, is contingent on the detection of these effects. In cases where the energy spectrum of the water surface is confined to wavelengths which are effectively damped by surface films, the average maximum tilt of the surface is sufficiently reduced so that proper choice of the viewing angle will completely eliminate images from within the slick area. In this case the slick can be detected with a signal-to-noise ratio which is nearly infinite. Where longer wavelengths that are not damped by the films are present, complete discrimination is possible only under those conditions where the loss of boundary resolution destroys the usefulness of the method.

To illustrate these effects, a series of three-component wave analogs is shown in Fig. 10. The curves were generated by combining three sine-wave inputs (ranging in relative amplitude from 0 to 1) to an oscilloscope (column A or B). The three input wavelengths were chosen to represent waves which are attenuated by factors of 1.0, 0.5, and 0.1 by a surface film, and such damping was simulated electrically. The undamped elevation profiles are shown in column C and the slope profiles in column E. The slope profiles were obtained by feeding the combined inputs through a simple RC differentiating circuit. The corresponding damped curves are shown in columns D and F. The spectral distribution of the original input amplitudes is shown in columns A and B, and the signal-to-noise ratios for four viewing angles is shown in column G. The ratios in column G are based purely on the number of images falling within the arbitrary acceptance angle bands representing approximately one-quarter of the maximum tilt angles encountered in Item 1 of the figure. These acceptance angles are much larger than would ordinarily be used, but the results are qualitatively in line with experimental observations.

The signal-to-noise ratios will vary slightly with the phasing of the wave's components. The general trend indicates that the signal-to-noise ratio improves as the viewing angle is moved away from zero, and the ratio then becomes infinite in all cases. However this is accompanied by a marked decrease in the number of reflections outside the slick area and a concentration of these images at the crest of the major components. Thus, the cost of improved ratios is the loss of background information against which the slick area may be compared.

In the light of the observed wind-related variations in the distribution patterns of surface slicks, this loss of background information becomes a factor of major importance. At low wind velocities, where the sea state is usually small, organic films tend to accumulate in areas having dimensions of hundreds to thousands of feet. As the wind velocity increases, these films tend to distribute in long wind-oriented streaks having dimensions on the order of tens to hundreds of feet. At higher wind velocities, where longer wavelengths can reasonably be expected, slicks usually stretch out in long, very narrow stripes which may be a few inches to a few feet in width. In this third state, the longer water waves often have dimensions which are large compared to the slick width; so the likelihood of detection decreases rapidly as the viewing angle is moved away from zero, with the resulting loss of background information density.

The intensity of individual facets has already been shown to be some function of the radius of curvature and, since an increase in the median radius of curvature is a necessary consequence of wave damping, those facets which reflect from within the slick area will, on the average, yield more intense images than those outside the slick area (Fig. 11). The consequence of this in terms of area-integrated density was suggested earlier. Under low sea state conditions, the slick area viewed at a facet tilt angle of zero degrees is invariably brighter than the background. As the viewing angle is moved away from zero

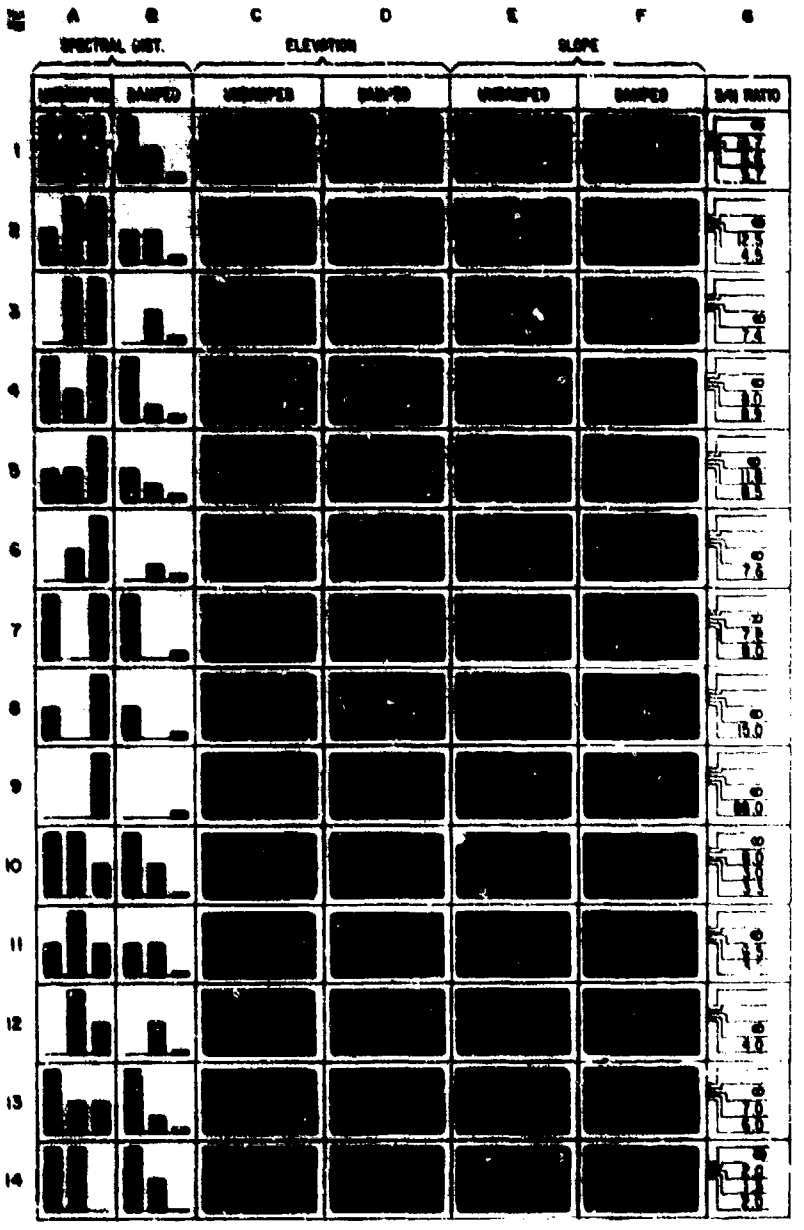

Fig. 10 – Sea-surface waveforms simulated by three-component sine-wave systems with and without damping. The spacing between each pair of horizontal lines at the left in column G represents an arbitrarily chosen value of the acceptance band $\omega_0 \pm \omega_a$.

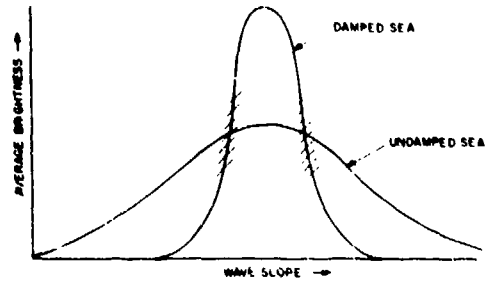

Fig. 11 – Relative plot of average brightness from damped and undamped sea as a function of wave slope

degrees, the number of these more gently curved facets which reflect light into the camera decreases. Over some range of viewing angles, the increase in intensity from the increased radius of curvature of individual facets is counterbalanced by the decrease in number, and the area-integrated intensity of light reflected from the slick is not significantly different from that reflected from the background. Beyond this critical zone, the number of long-radius facets which reflect into the camera falls toward zero, and the slick appears dark in contrast to the background.

When the characteristic slick dimensions have become small compared to the dimensions of major wave components, the probability of distinguishing slick areas on the basis of average slope becomes very small unless long exposure times can be used to integrate the information over a period at least equal to that of the longest wave components. A possibility remains, however, of using the average radius of curvature as an indicating parameter. Such a procedure would, in principle, require an area-by-area comparison of the intensity distribution of resolved facets and the replotting of the information to form a contrast-gradient map of the surface. Such a readout process requires a sophisticated data reduction system, but an approximation to this can be achieved by purely photographic processes which eliminate all images below an arbitrary intensity level. Some limited success has been obtained with this technique, which will be discussed later in the report.

EQUIPMENT AND TECHNIQUES

All water-surface photographs were taken with either a hand-held 35-mm still camera, a 35-mm Mitchel motion picture camera, or a CAS-2 aerial moving-film strip camera.

Framed motion pictures were taken with two Mitchel cameras mounted side by side in the transparent nose cone of a P2V-5 aircraft. The cameras were mounted on "top hat" mounts which permitted adjustment to any desired angle in relation to the solar elevation. The camera optical axes were parallel to the line of flight, which was in the direction of the azimuth angle of the sun. The mountings were not independently stabilized, so the field of view was subject to roll, pitch, and yaw of the aircraft.

Strip camera pictures were taken with the CAS-2 camera. This was mounted on an A28A gyrostabilized mount supported over a window cut into the tunnel hatch of a P2V aircraft (Fig. 12) or the radar hatch of an S2F aircraft. The stabilized mount provided both

Fig. 12 – CAS-2 strip camera on A28A gyrostabilized mount on tunnel hatch of P2V-5 aircraft

automatic compensation for aircraft roll and pitch and manual correction for drift. The limits of roll and pitch compensation are ±8 degrees, and the response characteristics were adequate when the aircraft was flown skillfully in air of low turbulence.

Modifications to the CAS-2 camera included a special single lens cone assembly which provided for (a) a pivot point for continuous adjustment of the viewing angle of the camera, (b) removal of the divider in the center of the slit assembly, (c) disablement of the automatic footage printing light, and (d) electrical provision for stepless adjustment of the depression angle compensation in the film-speed-control circuit.

A 240-mm Schneider Componon lens was used on the strip camera to give a transverse field of view of 53 degrees. In order to minimize the contribution of reflected skylight and light reflected from particulate matter or bubbles beneath the water surface, a dark-red F filter was usually used. Under poor light conditions, a somewhat less dense A filter was used for the same purpose.

All glitter photographs were taken with the aircraft flying in the direction of the azimuth angle of the sun and on a line which passed as nearly over the target area as possible. However, piloting difficulties often resulted in errors up to several hundred yards.

Eastman Kodak Plus-X Aerecon film was used for the strip photographs because of its wide latitude of exposure. The pictures shown later in this report were usually normal prints made from the film. Those designated as high contrast were made by a stepwise process. First, a high-contrast print was made of the original negative. This was then

rephotographed, using lithographic line film, and a high-contrast print was made from this. A second line negative was then prepared, and the final print was made on high-contrast paper. The final stages were made with very long exposure times to increase the size of the individual images by halation.

RESULTS

Framing Camera

Figure 13 shows photographs of a slick created on Chesapeake Bay by continuously dropping oleic acid from the platform shown at the right end of the slick. Because of the low sun angles (20° and 30°), the glitter pattern extends to the horizon and the most intense glitter arises from those areas of multiple reflections outside the primary reflection ellipse where reflections are accentuated by the near-grazing incidence.

The characteristic inversion in area-integrated density, which arises from the elliptical symmetry of the reflection pattern, is readily seen in the next to the last frame of Fig. 13 (b).

The image in Fig. 14 is at a greater photographic scale than in Fig. 13. This picture was taken at the same time as those of Fig. 13 (b) but with a longer focal length lens. The result of restricting the field of view to cover a narrower range of facet angles on the uniformity of the presentation is obvious. The relation of the reflections which occur within the slick area to the longer, undamped components of the water-wave structure is apparent in both the spacing and relative size of the reflections from within the slick. Attention is called to the circular refraction pattern of the waves surrounding the platform; this is caused by reflections from the piling structure which supports the platform.

The optical clarity of this particular kind of slick is abnormal because of the mode of its formation. By continuously supplying a surface-active material to the water surface, the normal dissipative losses were compensated and the slick maintained a dimensional coherence not usually found under the wind conditions (12-29 knots) which existed. Several zones of lighter and darker areas are also to be seen in Fig. 13; these are presumed to represent areas of greater and lesser concentrations of naturally distributed slick-forming materials. The basis for this presumption is that the position of these areas changed only slowly over a period of several hours. It would not be expected that either cloud shadows or velocity variations in the wind structure would exhibit this stability.

The usual distribution of slick-forming materials under high wind conditions is illustrated in Fig. 15. The scattered black streaks and patches represent slicks formed by the compression of surface-active materials at the convergent zones of water circulation patterns. The dimensions are very much smaller than the longer wave components but large enough in terms of the smallest wave components to give a reasonable discrimination. This situation is represented by item 2 of Fig. 10.

Figure 16 indicates the differences between slick and nonslick areas in a vertical flash picture where the photographic scale permits complete resolution of the individual facets. Note the increased size and intensity of facets from the damped waves.

The other extreme is indicated in Fig. 17 where the photographic scale is sufficiently large to eliminate all details of wave structure. The slicks shown are on the order of two miles in length and their distribution pattern suggests that the wind velocity was quite low.

Fig. 13 – Sequential framing camera photographs of glitter pattern from slick on Chesapeake Bay. Oleic acid slick was maintained by dripping oil from platform at right. Solar elevations were (a) 20 degrees and (b) 30 degrees. In each sequence from left to right, the airplane is approaching platform along the direction of solar azimuth angle.

Fig. 14 – Larger scale photograph of same condition shown in Fig. 13 (b)

Fig. 15 – Distribution of slicks (thin streaks) under high-wind conditions. Width of picture covers approximately 20 feet.

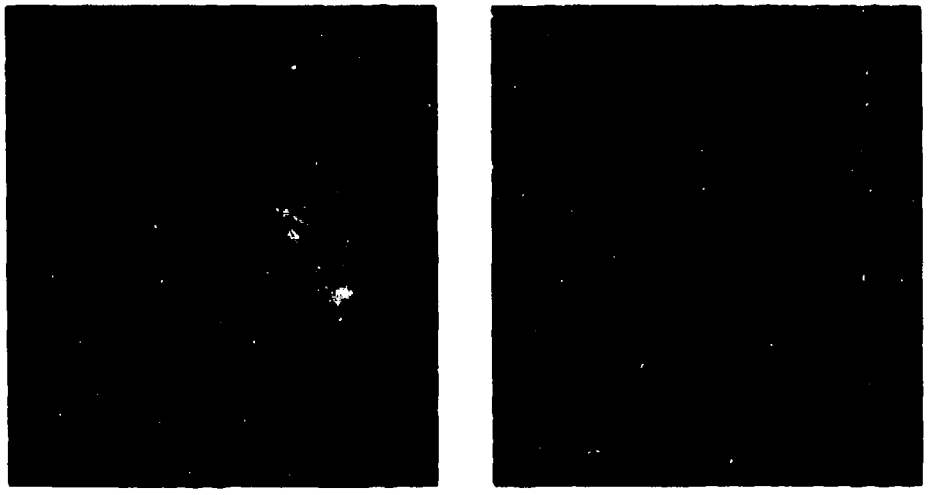

(a) (b)

Fig. 16 – Vertical flash photograph of (a) damped and (b) undamped water in tank. Camera elevation 60 inches; resolution 0.24 mm at surface.

Fig. 17 – Framing camera photograph of natural slicks and ship wake. Camera elevation 33,000 feet; resolution capability 4 meters.

The wake of a surface ship is indicated by the arrow. At the head of the arrow is a white streak representing one arm of the Kelvin wave system. The dark streak branching off from this is the turbulent wake. The inversion in optical density of this turbulent wake with its position in relation to the center of the distribution pattern clearly indicates that a decrease in average wave slope is responsible for its visibility. The other arm of the Kelvin wave pattern is only faintly visible.

Strip Camera

Typical strip camera pictures are shown in Figs. 18-21. Figure 18 indicates the appearance of slicks at sea states ranging from zero to four. Figure 19 illustrates the effect of viewing angle, Fig. 20 the effect of exposure time, and Fig. 21 the effect of time-sequence photography.

Figure 18 (a) indicates an essentially zero-wind zero-seastate condition in which the sea surface is almost a plane mirror, the wind velocity being too low to generate the capillary waves necessary to delineate the slick area. The only reflections recorded in the photograph (facet angle 2.5 degrees) are from a train of waves from a ship which passed about a mile from the target area. The images are surrounded by halations and many of them show long thin streaks. These streaks are probably reflections from the slit edges, though they may be associated with a secondary wave system on top of the ship's waves. Under these conditions optical detection of slicks is impossible.

The rest of the sequence in Fig. 18 shows the appearance of slicks at increasing wind velocities. Under the least rigorous conditions in which slicks could be detected (Fig. 18 (b)),

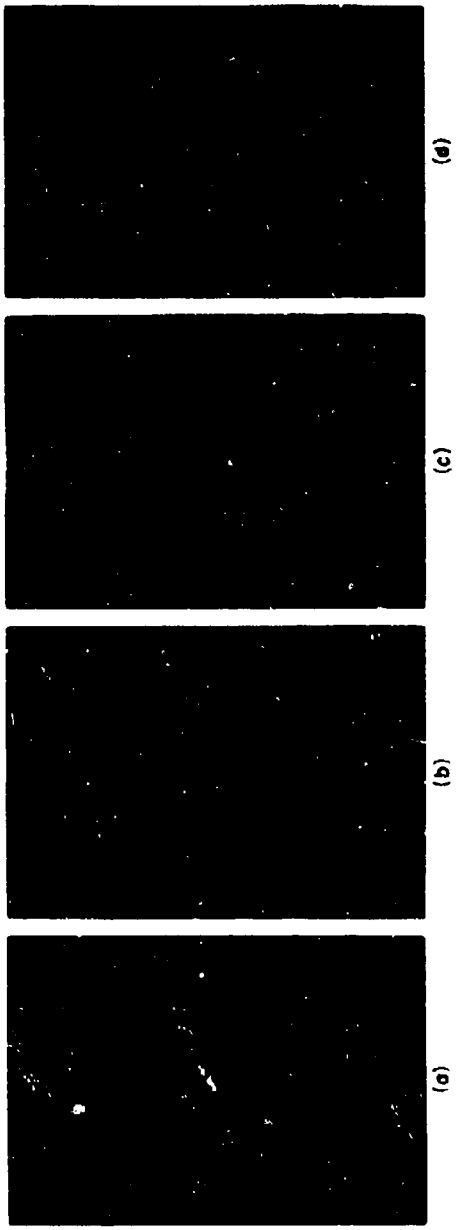

Fig. 18 – Strip camera photographs of Chesapeake Bay showing appearence of slicks at various wind conditions: (a) dead calm, (b) gusty breeze of about 6 knots, (c) 10-knot breeze, and (d) 15 to 18-knot breeze

(a)

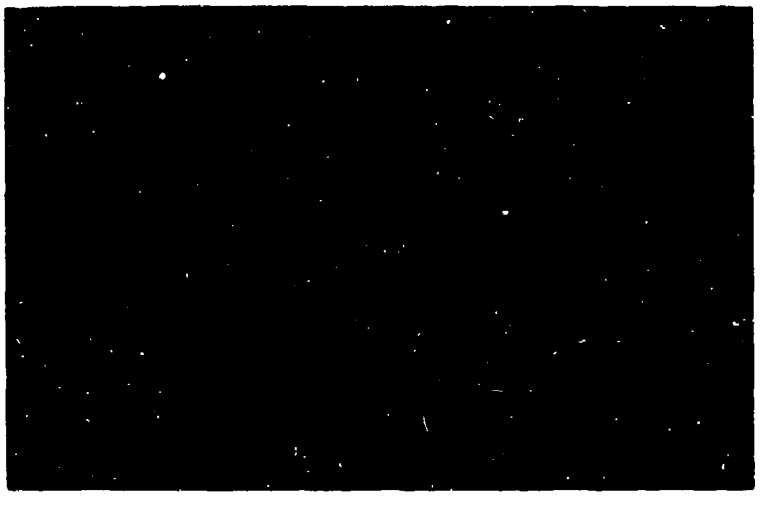

(b)

Fig. 19 – Ship-generated slicks in the Gulf of Mexico at viewing angles of (a) 2° and (b) 26°

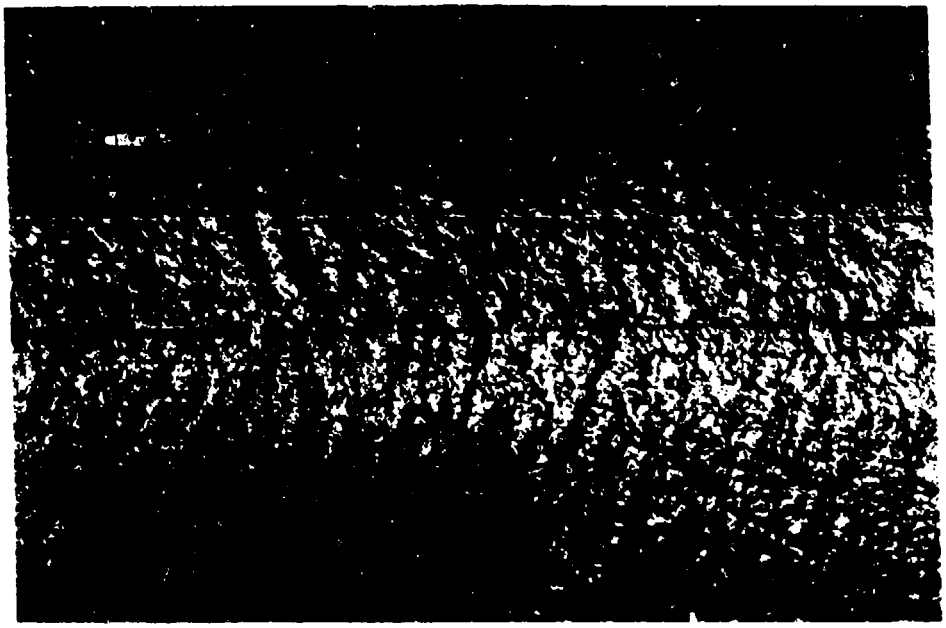

(a)

Fig. 20 – Strip camera photographs of glitter at exposure times of (a) 1/50 sec and (b) 1/3 sec. In (a) the arrows indicate the wake of a submarine which was traveling at a speed of 5 knots.

the distribution of the slicks shown was dominated by the turbulence generated by tidal flow past the bridge pilings. With a current of about one knot, these effects extended to a distance of at least 2000 yards downstream. As the wind picks up, its contribution to the distribution of slicks increases and the pattern changes (Fig. 18 (c)). At even higher wind velocities (Fig. 18 (d)), the wind effects become sufficient to severely limit slick detectability. In Fig. 18 (d) slicks are present but are drawn out into long, thin, scarcely detectable ribbons. In the original photograph these are visible, from a low viewing angle, in a direction roughly parallel to the wind, as long dark lines across the wave structure. The presence of these slicks was confirmed at the time the photograph was taken by visual observations from a small boat. The estimated width of individual lines ranged from 2 or 3 inches to about 18 inches.

The effects of extreme changes in viewing angle are illustrated in Fig. 19. In Fig. 19 (a) the lower slick visible was associated with a ship which remained adrift in the water for about 20 minutes, the upper with a second ship moving at about 5 knots. At a facet angle of about 2 degrees the slick stands out clearly from the background. At a facet angle of 26 degrees (Fig. 19 (b)) the slick is less distinguishable because of the loss of background information. At the steeper facet angle, the only reflections recovered seem to be associated with a system of long-crested waves having a wavelength of about 40 feet.

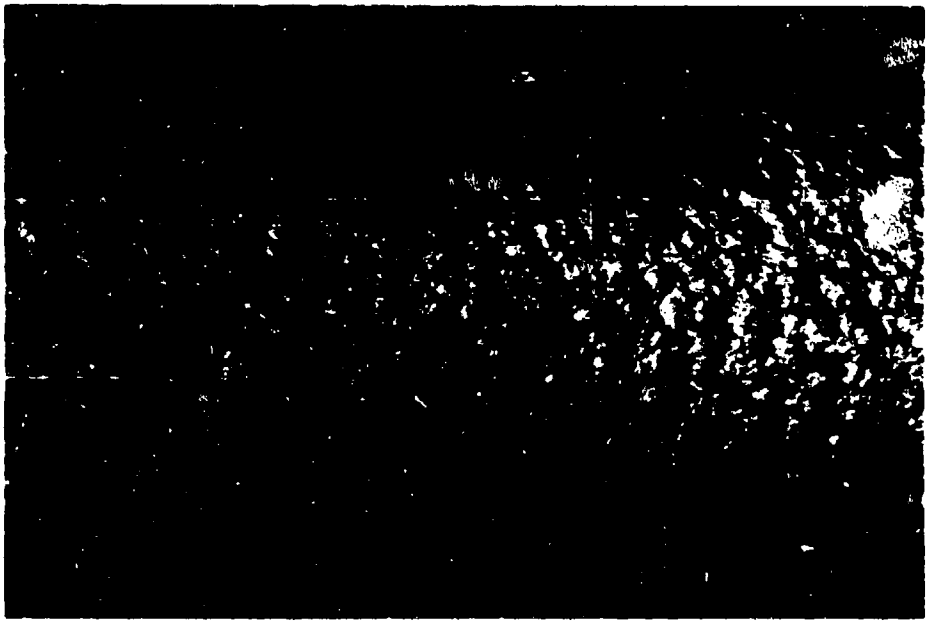

(b)

Fig. 20 (Cont'd) – Strip camera photographs of glitter at exposure times of (a) 1/50 sec and (b) 1/3 sec. In (a) the arrows indicate the wake of a submarine which was traveling at a speed of 5 knots.

The appearance of the images at two exposure times (1/50 and 1/3 sec) is shown in Fig. 20. Smoothing produced by the turbulent wake of a shallow submarine is faintly indicated by an increase in facet brightness and a decrease in the number of facets. These effects are accentuated by the longer exposure time.

Figure 21 represents a time sequence which illustrates the possibilities of the method for studying the time distribution of slicks.

The ability of high-contrast printing techniques to isolate the larger, brighter facets from areas of pronounced wave damping is shown in Figs. 22 and 23. The sequence shown in Fig. 22 shows the effect of printing a negative showing the track from a periscoping submarine at progressively higher degrees of contrast. In the original print (Fig. 22 (a)), the submarine trail can be detected only by close scrutiny of the details of the glitter pattern. With increasing density, the background gradually drops out, and the reflections directly associated with the turbulent smoothing of the water surface begin to stand out. With ultrahigh contrast, the arrangement of these becomes sufficiently unique to serve as an indicator of the track. Figure 23 shows the enhancement of smoothed areas both in the turbulent wake of a ship and in the smoothing caused by aerodynamic turbulence generated in the wind blowing across the ship. The sea state at the time was 3.

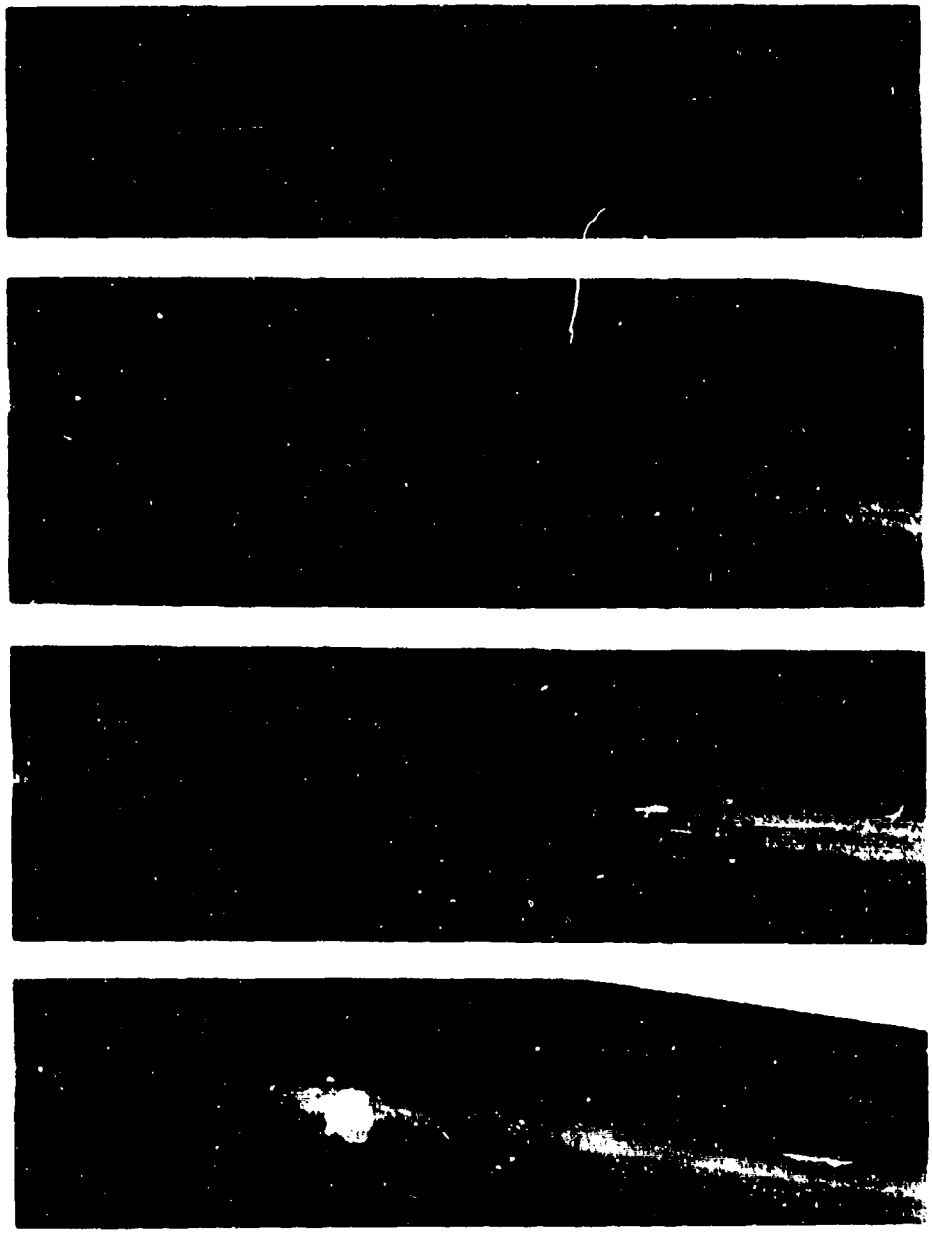

Fig. 21 – Strip camera time-sequence photographs showing smoothing in wake of turning ship. Photographs taken approximately five minutes apart and covering the same area.

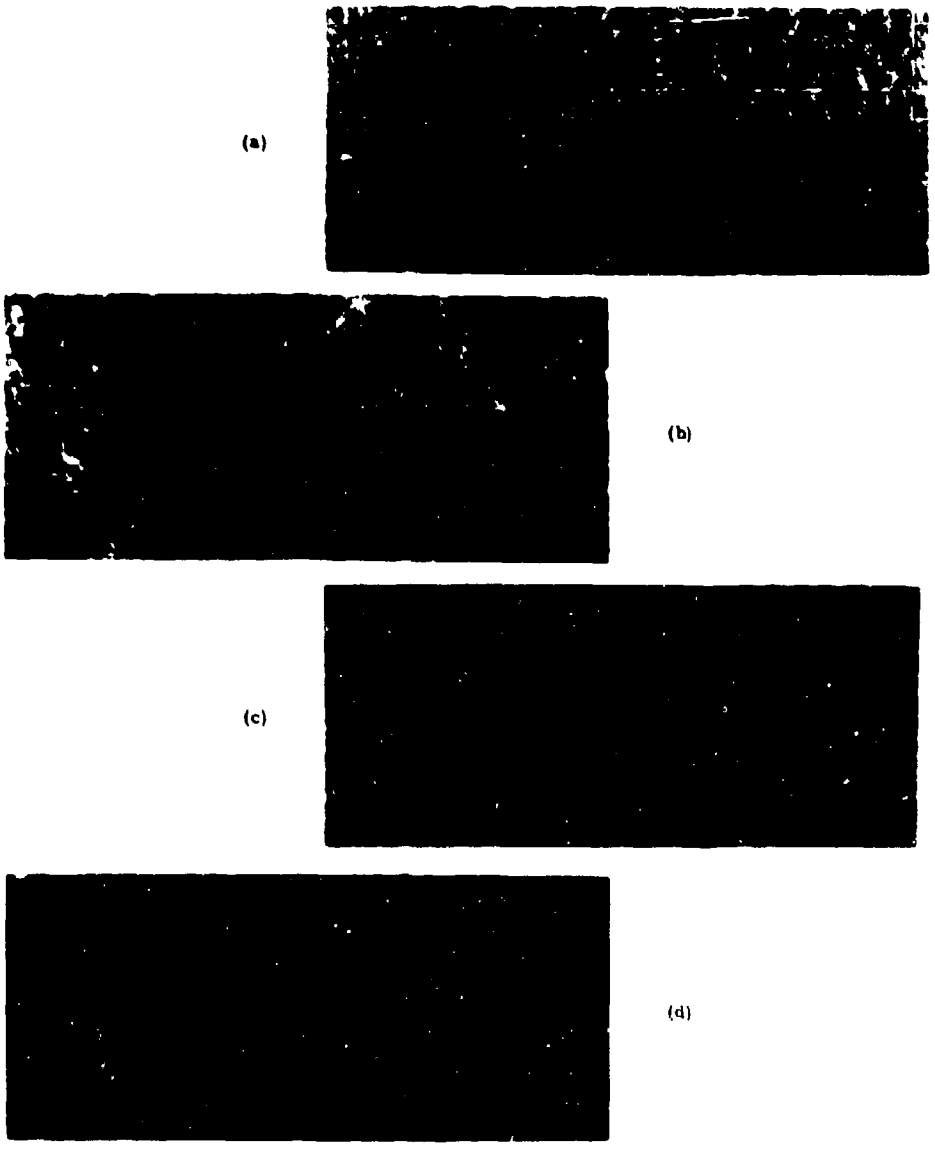

Fig. 22 – Submarine-generated wake of periscoping submarine (at left). (a) Normal print; (b), (c), and (d) ultrahigh-contrast prints. Width of photograph represents approximately one mile.

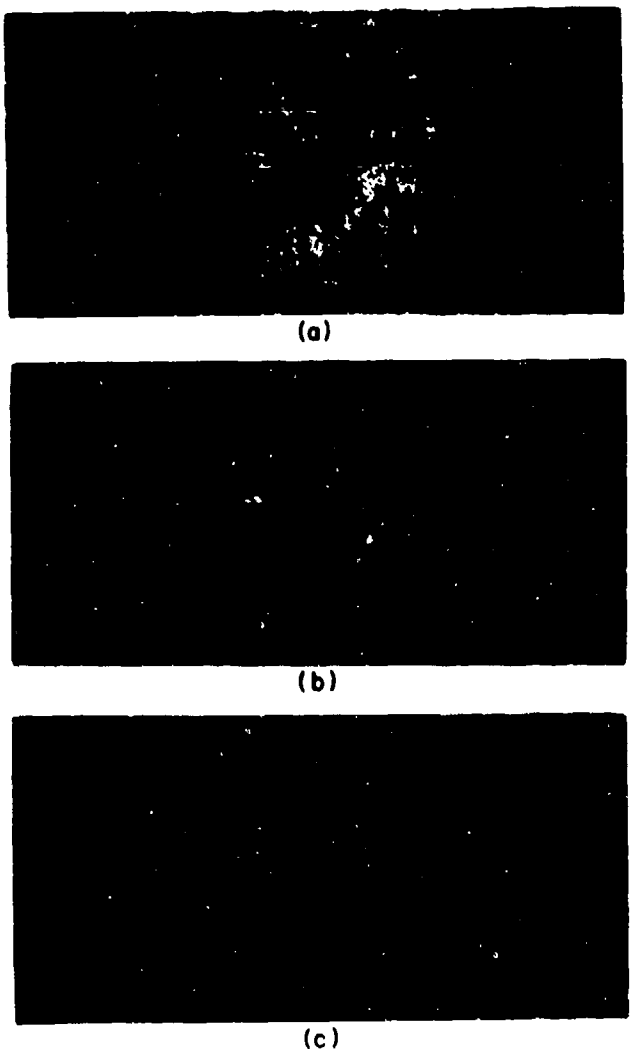

Fig. 23 – Wake of surface ship at sea state 3. (a) Normal print, (b) and (c) ultrahigh-contrast prints. Note hydrodynamic smoothing aft from turbulent wake and smoothing off starboard flank from interference of ship with the wind.

DISCUSSION

From both theoretical and observational results, it has been shown that the detection of slicks by sun-glitter photography is feasible under certain conditions of wind and sea state. It is equally obvious that some sea conditions made slick detection impossible, and others make it extremely difficult. These conditions are summarized briefly in Table 1.

Table 1
Weather Factors Affecting Slick Detection

Wind Speed (knots)	Sea State	Detection Probabilities	Most Significant Parameter
<2	0	Impossible	-
0- 6 and highly variable	0-1	Unreliable	Mean slope
4-10 and steady	0-2	Excellent	Mean slope
10-20	2-4	Difficult	Radius/slope
>20	4	Extremely difficult or impossible	Radius of curvature

The two optically significant parameters which are affected by slicks are the mean slope and the radius of curvature of the water surface. Where the major components of wave slope are associated with waves short enough to be damped by films, the use of mean slope as the indicating parameter is most effective. It is only in circumstances where major slope components are associated with relatively long waves that the radius of curvature must be used.

Where the slope can be used, the field of view should be restricted to wave facets of tilts that lie completely within or, preferably, completely outside of the crosshatched areas indicated in Fig. 11 to avoid the ambiguity associated with the density inversion transition zone. At present, the author knows of no way of anticipating the best viewing angle to meet these conditions. While the damping characteristics of a specific surface film at a specified film pressure can be fed into an analog or digital representation of a specific wave system to yield a specific answer for that system, the difficulty of matching the model to a specific sea remains. Variations of the slope spectra with the instantaneous wind conditions, prior history of the sea, fetch, local currents, and wind duration are relevant, but usually unknown, parameters. Current research programs are beginning to shed light on some of these effects and, with time, it is expected that an intellectually satisfying basis for choice of viewing angle will arise. In the meantime, a rough rule of thumb is to aim the camera at a facet angle representing one-half to two-thirds of the angular spread between the center of the reflection ellipse and the visual boundary of the reflection ellipse.

Where it is necessary to use radius of curvature as the sensitive parameter, the camera should be aimed to catch reflections from facets of near-zero tilt, since the increase in radius is usually associated with a decrease in the mean slope.

Thus far, a discussion of photographic scale has been avoided. It is apparent that the primary requisite is that the target image must be large in comparison to the limits of resolution. A corollary requirement is that the target image be small enough in relation to the total area surveyed so that it can be readily distinguished from the background. In cases where the slick areas are relatively large and slope can be used as the distinguishing parameter, the most favorable conditions would include very high camera altitudes and long lenses to restrict the field of view to a narrow range of facet angles. If the slick dimensions are sufficiently large compared to the longest wavelengths present, the scale could be sufficiently large to wipe out the details of wave structure, and the resulting patterns would give a clear, unambiguous presentation of the slick areas.

Problems in scale arise when the slick areas are small in comparison to the wave structure. In many cases, observed streaks of slick on the sea surface are only a few inches to perhaps a foot in width. In some cases, glitter photographs have been obtained of ship-generated slicks which were not more than 2 or 3 feet in width. Since these dimensions are small compared to ocean waves, the scale must be held to values which permit resolution on the order of a few inches so that enough background glitter is resolved to outline the slick areas. It is difficult to establish a rational basis for scale in this situation, and it is the author's experience that a scale which permits a resolution on the order of 2 inches or less seems to give satisfactory results. This degree of resolution leads to some confusion because of the details of wave structure which are included, but it does yield a negative which can be satisfactorily analyzed by ultrahigh-contrast printing processes and, presumably, by more sophisticated data analysis systems.

On the basis of observational results, exposure time seems to fall also into an indeterminate category. Satisfactory results have been obtained with times ranging from 1/1000 to approximately 1 second. Longer times give more integrated data, but this advantage is gained at the expense of resolution and the practical results obtained to date do not justify any dogmatic pronouncement on the question.

SUMMARY

The use of sun-glitter photography has been examined, tested, and found to be a highly useful tool for studying hydrodynamic smoothing and the distribution of surface films on water surfaces, provided that such films are sufficiently compressed to cause wave damping. The technique is most successful at sea states of 0 to 2 and wind velocities of 4 to 15 knots. It is of no value at wind velocities too low to cause capillary waves on the surface and is of limited value at sea states of 3 and above.

Through the use of ultrahigh-contrast printing processes, it has been possible to extend the usefulness of the method to include detection of hydrodynamic smoothing caused by the turbulent wakes of ships and submarines at sea states up to 4.

RECOMMENDATIONS

In view of the possible relevance of surface-chemical phenomena on the sea to the general problem of antisubmarine warfare (ASW), it is recommended that sun-glitter photography be used for additional studies in the following areas:

1. The effects of wind on the formation, distribution, and dissipation of natural and synthetic slicks.

2. The effects of water motions occurring naturally, or generated by moving ships and submarines, on the distribution of slicks.

3. Direct detection of hydrodynamic smoothing caused by submerged submarines.

While major improvements in the method itself are beyond the purview of the Chemistry Division, several possibilities which may deserve consideration are (a) the coupling of two television cameras or other line scanners at opposite ends of an aircraft, or in two separate aircraft, to permit use of correlation techniques in the data analysis, (b) the use of multiple slits on a single strip camera to increase the number of images without loss of resolution, and (c) the use of long-lens cameras mounted in high-altitude aircraft, balloons, or satellites to restrict the field of view to a limited range of facet angles without loss of area coverage.

The ultimate usefulness of this technique in ASW will probably be contingent on the development of greater understanding of the oceanographic and meteorologic phenomena which contribute to the optical appearance of the sea, the interaction of these phenomena with submarine-generated water movements, and the application of this information to more sophisticated scanning and readout systems. The use of sun-glitter photography as an experimental tool for the study of such phenomena is recommended.

ACKNOWLEDGMENTS

In 10 minutes of thought, the author was able to recall specific contributions of 27 individuals to the research programs on which this report is based. Their anonymous but very real assistance is very much appreciated. Particularly noteworthy contributions were made by W. A. Affens, J. D. Bultman, J. M. Leonard, C. Presbrey, and C. O. Timmons of the NRL Chemistry Division, P. Green and T. Robinson of the Technical Information Division, J. Milmer of the Engineering Services Division, and CDR Keister and LCDR C. Carroll of the Administrative Services staff. Especial thanks must go to D. Berryhill, TID, for his outstanding faithfulness to the project and his imaginative use of photographic techniques in developing the capabilities of the ultrahigh-contrast printing technique.

BIBLIOGRAPHY

1. Bigelow, H.B., and Edmondson, W.T., "Wind Waves at Sea, Breakers and Surf," Hydrographic Office Publication No. 602, Suitland, Md., 1947

2. Cox, C., and Munk, W., "Statistics of the Sea Surface Derived from Sun Glitter," J. Marine Res. 13(No. 2):198-227, 1954

3. Cox, C., and Munk, W., "Measurement of the Roughness of the Sea Surface from Photographs of the Sun's Glitter," J. Opt. Soc. Am. 44(No. 11):838-50, 1954

4. Cox, C., and Munk, W., "Some Problems in Optical Oceanography," J. Marine Res. 14(No. 1):63-78, 1955

5. Cox, C.S., "Measurement of Slopes of High-Frequency Wind Waves," J. Marine Res. 16(No. 3):199-225, 1958

6. Defant, A., "Physical Oceanography," New York:Pergamon Press, 1961

7. Duntley, S.Q., "Measurements of the Distribution of Water Wave Slopes," J. Opt. Soc. Am. 44(No. 7):574-5, 1954

8. Lamb, H., "Hydrodynamics," 6th ed., New York:Dover, 1945

9. Longuet-Higgins, M.S., "The Statistical Distribution of the Curvature of a Random Gaussian Surface," Proc. Cambr. Phil. Soc. 54(Pt. 4):439-53, 1958

10. Longuet-Higgins, M.S., "The Distribution of the Sizes of Images Reflected in a Random Surface," Proc. Cambr. Phil. Soc. 55(Pt. 1):91-100, 1959

11. Longuet-Higgins, M.S., "Reflection and Refraction at a Random Moving Surface. Part I, Patterns and Paths of Specular Points. Part II, Number of Specular Points in a Gaussian Surface. and Part III, Frequency of Twinkling in a Gaussian Surface," J. Opt. Soc. Am. 50(No. 9):838-56, 1960

12. Longuet-Higgins, M.S., and Stewart, R.W., "Changes in the Form of Short Gravity Waves on Long Waves and Tidal Currents," J. Fluid Mech. 8:565-83, 1960

13. Longuet-Higgins, M.S., and Stewart, R.W., "The Changes in Amplitude of Short Gravity Waves on Steady Non-Uniform Currents," J. Fluid Mech. 10:529-49, 1961

14. Munk, W.H., "High Frequency Spectrum of Ocean Waves," J. Marine Res. 14(No. 4): 302-314, 1955

15. Pierson, W.J., Jr., Neumann, G., and James, R.W., "Practical Methods for Observing and Forecasting Ocean Waves by Means of Wave Spectra and Statistics," Hydrographic Office Publication 603, 1955

16. Sandover, J.A., and Taylor, C., "Determination of the Profiles of Water Waves," J. Sci. Instr. 37(No. 4):141-5, 1960

17. Schooley, A.H., "A Simple Optical Method for Measuring the Statistical Distribution of Water Wave Slope," J. Opt. Soc. Am. 44(No. 1):37-40, 1954

18. Schooley, A.H., "Curvature Distributions of Wind-Created Water Waves," Trans. Am. Geophys. Union 36(No. 2):273-8, 1955

19. Schooley, A.H., "Facet Separation Distributions of Wind-Created Water Waves," Trans. Am. Geophys. Union 36(No. 6):933-4, 1955

20. Schooley, A.H., "Profiles of Wind-Created Water Waves in the Capillary-Gravity Transition Region," J. Marine Res. 16(No. 2):100-108, 1958

21. Schooley, A.H., "Short Fetch Water Wave Slope Probability Distributions," NRL Miscellaneous Paper No. 41, 1957

22. Schooley, A.H., "Probability Distributions of Water-Wave Slopes Under Conditions of Short Fetch," Trans. Am. Geophys. Union 39(No. 3):405-8, 1958

23. Schooley, A.H., "Double, Triple, and Higher-Order Dimples in the Profiles of Wind-Generated Water Waves in the Capillary-Gravity Transition Region," J. Geophys. Res. 65(No. 12):4075-9, 1960

24. Schooley, A.H., "Relationship Between Surface Slope, Average Facet Size, and Facet Flatness Tolerance of a Wind-Disturbed Water Surface," J. Geophys. Res. 66(No. 1): 157-62, 1961

25. Schooley, A.H., "Upwind-Downwind Ratio of Radar Return Calculated from Facet Size Statistics of a Wind-Disturbed Water Surface," Proc. IRE 50(No. 4):456-61, 1962

UNCLASSIFIED

Naval Research Laboratory. Report 6046 [CONFIDENTIAL, Grp. 3]. STUDIES OF THE OCEAN'S SURFACE. PART 3 - THE DETECTION OF SURFACE FILMS AND HYDRODYNAMIC SMOOTHING BY SUN-GLITTER PHOTOGRAPHY [Unclassified Title], by K.G. Williams. 31 pp. and figs., May 4, 1964.

The use of sun-glitter photography to detect monomolecular layers of organic material on water surfaces through their damping effect on short water waves is discussed. Since the method is nondiscriminating, damping caused by either aerodynamic or hydrodynamic effects is also detected. Two photographically relevant parameters are the slope and the radius of curvature of the water surface. Where the predominant slope components are associated with wavelengths short enough to be effectively damped, areas of compacted surface films

UNCLASSIFIED (over)

1. Monomolecular films – Detection
2. Ocean surfaces – Photographic anal.
I. Williams, K.G.

UNCLASSIFIED

Naval Research Laboratory. Report 6046 [CONFIDENTIAL, Grp. 3]. STUDIES OF THE OCEAN'S SURFACE. PART 3 - THE DETECTION OF SURFACE FILMS AND HYDRODYNAMIC SMOOTHING BY SUN-GLITTER PHOTOGRAPHY [Unclassified Title], by K.G. Williams. 31 pp. and figs., May 4, 1964.

The use of sun-glitter photography to detect monomolecular layers of organic material on water surfaces through their damping effect on short water waves is discussed. Since the method is nondiscriminating, damping caused by either aerodynamic or hydrodynamic effects is also detected. Two photographically relevant parameters are the slope and the radius of curvature of the water surface. Where the predominant slope components are associated with wavelengths short enough to be effectively damped, areas of compacted surface films

UNCLASSIFIED (over)

1. Monomolecular films – Detection
2. Ocean surfaces – Photographic anal.
I. Williams, K.G.

UNCLASSIFIED

Naval Research Laboratory. Report 6046 [CONFIDENTIAL, Grp. 3]. STUDIES OF THE OCEAN'S SURFACE. PART 3 - THE DETECTION OF SURFACE FILMS AND HYDRODYNAMIC SMOOTHING BY SUN-GLITTER PHOTOGRAPHY [Unclassified Title], by K.G. Williams. 31 pp. and figs., May 4, 1964.

The use of sun-glitter photography to detect monomolecular layers of organic material on water surfaces through their damping effect on short water waves is discussed. Since the method is nondiscriminating, damping caused by either aerodynamic or hydrodynamic effects is also detected. Two photographically relevant parameters are the slope and the radius of curvature of the water surface. Where the predominant slope components are associated with wavelengths short enough to be effectively damped, areas of compacted surface films

UNCLASSIFIED (over)

1. Monomolecular films – Detection
2. Ocean surfaces – Photographic anal.
I. Williams, K.G.

UNCLASSIFIED

Naval Research Laboratory. Report 6046 [CONFIDENTIAL, Grp. 3]. STUDIES OF THE OCEAN'S SURFACE. PART 3 - THE DETECTION OF SURFACE FILMS AND HYDRODYNAMIC SMOOTHING BY SUN-GLITTER PHOTOGRAPHY [Unclassified Title], by K.G. Williams. 31 pp. and figs., May 4, 1964.

The use of sun-glitter photography to detect monomolecular layers of organic material on water surfaces through their damping effect on short water waves is discussed. Since the method is nondiscriminating, damping caused by either aerodynamic or hydrodynamic effects is also detected. Two photographically relevant parameters are the slope and the radius of curvature of the water surface. Where the predominant slope components are associated with wavelengths short enough to be effectively damped, areas of compacted surface films

UNCLASSIFIED (over)

1. Monomolecular films – Detection
2. Ocean surfaces – Photographic anal.
I. Williams, K.G.

can be detected with a nearly infinite signal-to-noise ratio. Where major slope components are associated with longer waves not susceptible to damping, the signal-to-noise ratio deteriorates. Under adverse ocean conditions, changes of the average radius of curvature can sometimes be used to indicate areas of damping which are otherwise not readily detected.

UNCLASSIFIED

can be detected with a nearly infinite signal-to-noise ratio. Where major slope components are associated with longer waves not susceptible to damping, the signal-to-noise ratio deteriorates. Under adverse ocean conditions, changes of the average radius of curvature can sometimes be used to indicate areas of damping which are otherwise not readily detected.

UNCLASSIFIED

can be detected with a nearly infinite signal-to-noise ratio. Where major slope components are associated with longer waves not susceptible to damping, the signal-to-noise ratio deteriorates. Under adverse ocean conditions, changes of the average radius of curvature can sometimes be used to indicate areas of damping which are otherwise not readily detected.

UNCLASSIFIED

Naval Research Laboratory
Technical Library
Research Reports Section

DATE: January 1, 2001

FROM: Mary Templeman, Code 5227

TO: **Code 6100 Dr Murday**

CC: Tina Smallwood, Code 1221.1 1/3/2001

SUBJ: Review of NRL Reports

Dear Sir/Madam:

1. Please review NRL Report FR-6046 for:

☑ Possible Distribution Statement
☑ Possible Change in Classification

Thank you,

Mary Templeman

Mary Templeman
(202)767-3425
maryt@library.nrl.navy.mil

The subject report can be:

☑ Changed to Distribution A (Unlimited)
☑ Changed to Classification _____
☐ Other:

Signature Date 1/8/01

It is my opinion that this document can be changed to Distribution A. However, the Remote Sensing Division might want this division as well

This document can be declassified. It contains no information that has not been in open literature. It contains no information with critical national security importance

P R Lee

Code 7210 1/3/01

-- 1 OF 1
-- 1 - AD NUMBER: 350190
-- 2 - FIELDS AND GROUPS: 8/3, 14/4, 17/5
-- 3 - ENTRY CLASSIFICATION: UNCLASSIFIED
-- 5 - CORPORATE AUTHOR: NAVAL RESEARCH LAB WASHINGTON D C
-- 6 - UNCLASSIFIED TITLE: STUDIES OF THE OCEAN'S SURFACE. PART 3.
-- THE DETECTION OF SURFACE FILMS AND HYDRODYNAMIC SMOOTHING BY SUN-
-- GLITTER PHOTOGRAPHY
-- 8 - TITLE CLASSIFICATION: UNCLASSIFIED
-- 9 - DESCRIPTIVE NOTE: INTERIM REPT.,
--10 - PERSONAL AUTHORS: WILLIAMS,K. G. ;
--11 - REPORT DATE: 4 MAY 1964
--12 - PAGINATION: 31P MEDIA COST: $ 7.00 PRICE CODE: AA
--14 - REPORT NUMBER: NRL-6046
--20 - REPORT CLASSIFICATION: CONFIDENTIAL
--23 - DESCRIPTORS: (*MONOMOLECULAR FILMS, DETECTION), (*OCEANS,
-- SURFACES), PHOTOGRAPHIC ANALYSIS, ORGANIC MATERIALS, CAMERAS,
-- CHESAPEAKE BAY, SIGNAL-TO-NOISE RATIO, DAMPING, OPTICS, WATER WAVES
--24 - DESCRIPTOR CLASSIFICATION: UNCLASSIFIED
--27 - ABSTRACT: THE USE OF SUN-GLITTER PHOTOGRAPHY TO DETECT
-- MONOMOLECULAR LAYERS OF ORGANIC MATERIAL ON WATER SURFACES THROUGH
-- THEIR DAMPING EFFECT ON SHORT WATER WAVES IS DISCUSSED. SINCE THE
-- METHOD IS NONDISCRIMINATING, DAMPING CAUSED BY EITHER AERODYNAMIC

-